General-Purpose Gamut-Mapping Algorithms: Evaluation of Contrast-Preserving Rescaling Functions for Color Gamut Mapping

Gustav J. Braun and Mark D. Fairchild***

Munsell Color Science Laboratory
Chester F. Carlson Center for Imaging Science
Rochester Institute of Technology
Rochester, New York

Abstract

Experiments were performed to test a set of general-purpose gamut-mapping functions. These gamut-mapping algorithms utilized contrast-preserving scaling functions. These algorithms were tested against the GCUSP gamut-mapping algorithm proposed by Morovic and Luo,[1] which was shown to have very good "universal" gamut-mapping characteristics. The results of these experiments showed that vast improvements were obtained when linear lightness and chroma rescaling functions were replaced with contrast-preserving lightness and chroma rescaling functions. For these experiments, the gamut mapping consisted of sigmoidal lightness-remapping functions[2,3] followed by either "knee" functions[4,5] or "sigmoid-like" chromatic compression functions.

Current affiliation: Eastman Kodak Company, Rochester, New York.

Introduction

The need for color gamut mapping arises from the differences that exist in the color gamuts of imaging devices. For example consider the case shown in Figure 1. The CIELAB color gamut of the thermal printer is different from the color gamut of the monitor. As such, it is not possible to reproduce the colorimetry of all colors contained within the monitor gamut on a print generated from the thermal printer. There is a lack of universal intersection between the set of colors that are producible on the monitor and the set of colors that are producible on the thermal printer. As such a color **gamut-mapping algorithm** is required to map the **out-of-gamut** monitor colors into the color gamut of the thermal printer.

The importance of color gamut mapping as a fundamental component of the color imaging chain has been brought to the forefront in recent years with the formation of the Commission Internationale de L'Eclairage (CIE) Technical Committee 8-3. Specifically, research has begun to address the need for a "universal approach" to color gamut mapping.[6] Researchers have approached the gamut-mapping problem from different directions. Some of these solutions have been very complex, as with Kodak's UltraColor color gamut morphing[7] and the categorical gamut-mapping strategy presented by Motomura.[8] Others have been relatively straightforward, as with linear chroma compression toward a centroid point by MacDonald.[9] Each of these techniques was

designed to exploit or preserve characteristics of the original scene that were thought to be most important to the overall composition of the reproduction.

Much of the focus in gamut-mapping research has been on the chromatic image content while often overlooking the lightness characteristics of the gamut-mapped reproductions. Throughout a majority of the gamut-mapping literature, linear lightness-compression schemes have been reported. A recent modification to this process by Morovic and Luo[1] weights the lightness scaling such that more lightness compression was performed on low chroma colors than higher chroma colors. However, the form of this rescaling function still results in 100-percent linear lightness compression along the neutral axis (and proportionately less lightness compression for chromatic colors). They followed the chroma-weighted lightness rescaling with linear chroma compression toward the gamut **cusp**[**] while preserving metric hue in CIECAM97s color space.[10] This algorithm is referred to as GCUSP.

Linear scaling for both lightness and chroma has serious implications on the overall lightness and chromatic contrast in the final reproductions. Linear lightness compression globally lightens and globally reduces the lightness contrast of the rescaled image. This is particularly objectionable when the lightness dynamic range is very different between the source and destination gamuts. Linear chroma compression reduces chromatic contrast equally in both high and low chroma regions. The implication of this is that lower chroma features such as flesh tones are objectionably "washed out." Gamut-mapping research

[**] The gamut cusp point refers to the achromatic point of with the same lightness as the point on the gamut surface with the maximal chroma a function of hue angle.

performed by Gentile, Walowit, and Allebach,[3] Montag and Fairchild,[5] Stone and Wallace,[11] and Braun and Fairchild[12] has shown that knee functions or soft compression functions perform well for chromatic compression. These functions preserve the colorimetry of the lower chroma features, such as flesh tones, and compress the higher chroma colors more to fit within the destination gamut.

Pictorial Image Gamut Mapping Philosophy

The philosophy of the gamut-mapping algorithms presented in this research was to preserve, as accurately as possible, the hue, the lightness contrast, and the chromatic contrast of the original scene. In order to do this, several key gamut-mapping components were assembled.

Color Space

The linearity of hue in a color space is very important to gamut mapping. Both the CIELAB color space and the color space defined by CIECAM97s are nonlinear with respect to perceived hue lines, Figure 2a,b. The color space used for gamut mapping in this study was the Hung and Berns hue-linearized CIELAB color space described by Braun, Ebner, and Fairchild.[13] This color space is identical to CIELAB except in the "blue" region of color space where perceived hue lines significantly depart from metric hue angle of CIELAB. The importance of hue linearity has been evidenced by the recent interest of others in this area.[14-17] The advantage of using the Hung and Berns[12] data to correct the CIELAB color space is that their data set extends to more chromatic colors than the Munsell data used in the work by Marcu[14] and McCann.[15] This is important, since most gamut compression happens on high chroma colors where the hue non-

linearity is the greatest. An alternate color space would have been the IPT color space developed by Ebner and Fairchild,[18] but at the time this study was performed, it was not fully tested for pictorial image gamut mapping.

Lightness Contrast

Some of the common techniques used to overcome the lightness dynamic-range differences between an input and output gamut are shown in Figure 3. In general, all of the scaling functions shown in Figure 3 result in reproductions with reduced lightness contrast. The mean lightness of the scene is increased and the global image contrast is reduced because of the range compression. In the case of the hard clipping, all values below the cutoff lightness are reproduced as the same lightness. When the dynamic-range difference between the source and destination gamuts is large, hard clipping results in a "flattening" (loss of detail, shape, and texture) and lightening of the shadowed regions. The knee-function and the soft-clipping compression techniques work reasonably well for maintaining the lightness contrast of the original scene when the dynamic-range difference between the source and destination gamuts is small. However, for larger differences, they do not maintain the apparent contrast of the scene.

For matching applications, such as proofing, it is of the utmost importance to preserve the lightness contrast of the original in the mapped image. Linear lightness rescaling functions cannot achieve this. Recent gamut-mapping experiments have shown that, to avoid a loss in perceived lightness contrast, the lightness contrast of the original scene must be increased before the dynamic-range compression is applied to fit the input lightness range into the destination gamut.[2,3,12]

In these experiments, image-dependent sigmoidal lightness scaling functions were utilized. The form of these remapping functions was shown to be a function of both the image composition and dynamic-range difference between the source and destination devices.[2,3,19,20] While those described by Holm[19,20] were intended to produce an enhanced reproduction, the lightness remapping functions designed by Braun and Fairchild[2,3] were designed to match the lightness contrast of the original. These functions were derived from psychophysical lightness adjustment experiments, in which observers produced visual matches to a full dynamic-range original under reduced dynamic-range conditions. The sigmoidal remapping functions shown in Figure 4a,b illustrate the change in the remapping functions with changes in image content and the dynamic-range difference between the source and destination devices. Thus, more contrast and low-lightness compression is required to maintain the perceived contrast as the output dynamic range decreases.

Chromatic Contrast

In the experiments performed in this study, three types of contrast-preserving chromatic-rescaling functions were used to scale the input image colors into the destination gamut: a knee function given by Gentile, Walowit, and Allebach,[4] a "sigmoid-like" function termed ENHANCE, and linear chromatic compression. These functions are shown in Figure 5. As with Morovic and Luo's GCUSP algorithm,[1] the scaling direction was toward the cusp point for each hue angle.[***] The knee-function chroma-scaling technique preserves the chromatic contrast better than linear chroma compression because

[***] Cusp point scaling was selected based on its overall performance in the studies by Morovic and Luo.[1]

chromatic features are unchanged between the neutral axis and the knee point. The knee-point was set at the 90-percent point of the range from the cusp point to the destination gamut based on the good performance of the clipping algorithms shown by Montag and Fairchild.[5] Knee-function scaling is preferable to clipping since it reduces artifacts caused by mapping many input colors to one output color.

The ENHANCE "sigmoid-like" rescaling function has three linear regions: Region 1 - colorimetric; Region 2 - mid-chroma boost; and Region 3 - chroma compression. The first region was designed to preserve the low-end contrast and colorimetry by mapping the input chroma equal to the output chroma. The middle region was designed to increase the chroma of the mid-chroma features to help overcome the loss in chromatic contrast associated with the gamut-mapping process. The final region was designed to compress the out-of-gamut high chroma features into the destination gamut.

Gamut Mapping Order

In general, there are two ways in which the gamut of an image can be compressed. Assuming that the hue of the original colors are to be preserved, the lightness and the chroma of the colors can be compressed **simultaneously** or **sequentially** (usually lightness is compressed first then chroma). For the applications of proofing and matching, it is assumed that lightness rendition of the scene is more important than chromatic rendition. More information about lighting. shading, and feature composition are attributed to the lightness contrast of the scene than the chromatic contrast. As such, the first gamut compression operation that was performed was lightness dynamic-range compensation. This was then followed by chromatic dynamic-range compression. In

general, it was felt that performing simultaneous compression of the lightness and chroma would make it more difficult to control the exact form of the lightness compression. By following the lightness compression with chromatic compression that allows the lightness of the color to vary, the form of the original lightness compression function is modified. However, if the chromatic compression is applied more heavily near the edges of the color gamut than toward the achromatic axis, the form of the original lightness mapping function is better maintained for the near neutral colors. This is important since these colors represent the base composition of the scene. As such the sequential mapping process maintains the lightness contrast of the lower chroma colors while slightly sacrificing the form of the overall lightness mapping of the higher chroma colors.

Experimental

A series of gamut-mapping experiments were performed to test seven general-purpose gamut-mapping algorithms. These algorithms fit into three classes: 1.) *device-dependent gamut mapping* in which the gamut-mapping decisions are based on the similarity between the source and destination device gamuts; 2.) *image/device-dependent gamut mappings* in which the lightness remapping functions are based on the lightness content of the input image histogram, while the chroma mapping decisions are based on the device gamut boundary shapes; and 3.) *image-dependent gamut mapping* where all of the gamut-mapping decisions are based on input image gamut and the shape of the destination gamut.[10] These algorithms are listed in Table 1.

Monitor-to-Printer Experiment

The first experiment simulated the case where a full dynamic-range monitor original was mapped into the gamut of a Hewlett Packard HP870Cxi inkjet printer loaded with plain paper. The black point of the inkjet printer was 18 CIELAB L* units and the entire gamut of the printer essentially fit within the gamut of the monitor, Figure 6a,b.

To avoid differences in cross-media viewing conditions, these experiments were performed entirely using the monitor display. (Note: Only the final viewing of the gamut-mapped images was simulated. The shapes of the monitor and printer gamuts were real.) This eliminated both viewing-condition effects (e.g., mode of viewing and incomplete chromatic adaptation) and media differences (e.g., granularity, gloss, and resolution) that affect the appearance of the reproductions.

Twenty observers performed a paired-comparison matching experiment for the monitor-to-printer case. The observers were instructed to select the reproduction that was the closest match to the original. Seven different images were tested containing a wide range of scene content.

Printer-to-Printer Experiment

For the printer experiment, four print original images were gamut mapped into two destination printer gamuts. These four images were different from those used in the monitor-to-printer experiment. The output devices were the Xerox Regal MajestiK continuous-tone electrophotographic printer and the Xerox Xpress large-format ink-jet printer, both on plain paper. These printers represent typical graphic arts printers. The

Regal MajestiK printer has a lightness dynamic range of approximately 15 to 100 CIELAB L* units, and the Xpress printer has a lightness dynamic range of approximately 22 to 100 CIELAB L* units. The dynamic range of the Fujix Pictrography 3000 printer used to generate the hardcopy originals is approximately 6 to 100 CIELAB L* units using glossy paper (Note: The colorimetry was normalized to the luminance of the paper white.) The images were viewed under a fluorescent D50 source. The observers' task was to rank the reproductions with respect to how well they matched the original image. This experiment included 10 observers. Preference was not considered in these experiments.

As with the previous monitor-to-printer simulation experiment, the viewing conditions between the original and the reproduction were made as similar as possible, in this case by using prints for the original and reproductions. Gloss, granularity, and resolution differences could not be fully eliminated. In addition, the output devices were characterized for CIE Standard Illuminant D50 rather than the viewing source of fluorescent D50. This was due to limitations of the characterization software. This resulted in some illuminant metamerism that affected the accuracy of the colorimetric characterization. Despite these conditions, the differences among the various gamut-mapping algorithms could be clearly seen.

The SIG_CLP algorithm was eliminated from this experiment, due to its similar characteristics and performance to the SIG_KNEE algorithm, found in the monitor-to-printer experiment. This similarity was expected based on the location of the knee point in the SIG_KNEE algorithm at 90-percent of the destination gamut surface.

Printer-to-Printer Experiment: Softproofing

The third visual experiment consisted of a printer-to-printer gamut-mapping experiment. Twenty-one observers performed a paired-comparison experiment, in which they were instructed to choose the reproduction that was most similar to the original.

The original images consisted of nine prints from the Fujix Pictrography 3000 printer. The reproduction device was the Xerox Xpress inkjet printer using plain paper. The images consisted of both standard portrait and landscape scenes, as well as several more artistic images. For these scenes, there were fewer memory features on which the observers could base their decisions. In this experiment, the LIN_LIN algorithm was not used based on poor previous performance, and the SIG_CLP algorithm was not used because of its similarity to SIG_KNEE algorithm.

One additional algorithm was added to this experiment. The algorithm denoted as GENERIC consisted of an image-independent sigmoidal lightness remapping followed by hue-preserving cusp-point knee scaling. Essentially this algorithm was identical to the SIG_KNEE algorithm except that the lightness scaling function was the same for all of the images. The form of the GENERIC lightness scaling was taken from the normal lightness class given by Braun and Fairchild.[2,3] This algorithm was added to test the utility of performing sigmoidal-lightness scaling in an image-independent manner; such an approach is more amenable to color-management processes that use static device profiles, such as International Color Consortium (ICC) format profiles.

This experiment was very similar to the previous print-to-print experiment except the images were viewed as softproofs on a monitor, instead of using physical prints. Softproofs of the reproductions were utilized for two reasons. First, there was considerable metamerism that resulted from difference of the light source from CIE Standard Illuminant D50. Second, there were printer artifacts, in the form of halftone quantization, that masked many of the subtle differences in the gamut-mapping algorithms.

In order to generate the softproofs, some CIELAB values of the original Fujix prints and the Xpress reproductions were clipped to surface of the monitor gamut. This process did not result in any noticeable changes in appearance of the images. The Xpress gamut essentially fit within the monitor gamut, Figure 7a,b necessitating very little clipping. While the Fujix printer gamut had regions that were significantly higher in chroma than the monitor gamut, most of the images did not contain many features in these regions.

Results

A series of interval scales, shown in Figures 8-10, were developed that defined both the rank ordering of the algorithms performance and a gauge of the relative differences among the gamut-mapping techniques. For the paired comparison experiments, the scales in Figures 8 and 10 were generated using Thurstone's "Law of Comparative Judgments."[21] Incomplete matrix calculations were applied to cases of unanimous agreement among observers, in which cases it was impossible to directly calculate the Z-scores. The rank data associated with the printer-to-printer comparisons of the second experiment, Figure 9, were converted to interval scale data using the "Comparative-

Judgement Method of Data Reduction."[22] The error bars shown on these plots represent the visual uncertainty among the algorithms. If the mean Z-score of an algorithm is contained within the error bars of another algorithm, the two algorithms have statistically the same visual difference from the original. The confidence intervals, C, shown as error bars in the figures were calculated by C=1.386/sqrt(N), where N equaled the number of observers for the given experiment.

Evaluation of the interval scales indicated that, across the different gamut-mapping experiments, the algorithms could be grouped into three significantly different categories. The first category of algorithms was the device-dependent linear lightness and linear chroma compression. This category included the GCUSP_LIN and the LIN_LIN algorithms. For all of the images, these algorithms had much lower scale values than the images mapped using the sigmoidal lightness functions. This was primarily due to their low visual contrast, which resulted from the linear dynamic-range mapping.

The second category of results consisted of those images that were mapped using the sigmoidal lightness remapping functions and the linear chroma compression, SIG_LIN. This gamut-mapping strategy created significantly better matches than the first category. This result stressed the importance of faithful reproduction of the lightness contrast of the scene, which was not found with straight linear lightness reproduction.

The third category of algorithms consisted of those algorithms that utilized both the sigmoidal lightness remapping functions and the non-linear chroma compression functions (SIG_KNEE, SIG_CLP, GENERIC, SIG_IMGGAM, SIG_ENHANCE). These

techniques produced significantly better matches for all of the images than those produced by the first and second categories of algorithms. There were no significant differences noticed among these four algorithms. These gamut-mapping routines resulted in very similar images since the knee point of the mappings was set at 90-percent of the input gamut range (very similar to cusp-point clipping). The knee-point was set at the 90-percent point of the destination gamut based on the good performance of the clipping algorithms shown by Montag and Fairchild[5] combined with the added flexibility to reduce the possible artifacts of clipping.

One of the interesting results of the third experiment was that the GENERIC algorithm performed as well, on average, as the image-dependent SIG_KNEE and ENHANCE algorithms. This result suggests that it is possible to create a generic "profile" that could be used for all input images. The profile would be specific for a given destination dynamic range, but general for all input scenes. This would be very useful for implementation of these gamut-mapping algorithms in the framework of ICC color management. However, under extreme conditions it may still be more beneficial to use the image-dependent form of the sigmoidal-lightness remapping functions since is performs a tailored amount of compression in the highlight and shadowed regions of the particular scene.

The results of these experiments also support the use of simulated viewing conditions for evaluation of gamut-mapping algorithms to avoid the viewing condition problems of cross-media experiment. The results for the monitor viewing experiments were identical to those that utilized reflective samples. This type of experiment allows for the gamut-

mapping algorithms to be evaluated without confounding the analysis with viewing condition effects.

Conclusions

The gamut-mapping approaches that utilized sigmoidal lightness mapping followed by knee-function chromatic compression, similar to cusp-point clipping, performed best among the various gamut-mapping cases studied. These algorithms had general success due in large part to the tone-preserving nature of the sigmoidal lightness remapping functions. In addition, performing the chromatic compression using scaling functions that maintain chromatic contrast was highly beneficial compared to linear chromatic compression. Evidence was given for using a generic gamut-mapping algorithm that could be encoded into a profile, like those used in ICC color management.

Acknowledgements

The authors wish to thank Karen Braun and Raja Balasubramanian from the Xerox Corporation for their support in supplying calibrated prints for these experiments.

References

1. J. Morovic and M.R. Luo, Verification of Gamut Mapping Algorithms in CIECAM97s Using Various Printed Media, *Proceedings of 6th IS&T/SID Color Imaging Conference,* Scottsdale: 53-61 (1998).

2. G.J. Braun and M.D. Fairchild, Image Lightness Rescaling using Sigmoidal Contrast Enhancement Functions, *IS&T/SPIE Electronic Imaging '99, Color Imaging: Device Independent Color, Color Hardcopy, and Graphic Arts IV*, San Jose: 96-105 (1999).

3. G.J. Braun and M.D. Fairchild, Image Lightness Rescaling using Sigmoidal Contrast Enhancement Functions, *J. Electronic Imaging,* **8**: 380-393 (1999).

4. R.S. Gentile, E. Walowit, and J.P. Allebach, A Comparison of Techniques for Color Gamut Mismatch Compensation, *Journal of Imaging Tech.*, **16**: 176-181 (1990).

5. E.D. Montag and M.D. Fairchild, Psychophysical Evaluation of Gamut Mapping Techniques Using Simple Rendered Images and Artificial Gamut Boundaries, *IEEE Trans. Image Proc.*, **6**: 997-989 (1997).

6. J. Morovic, *To Develop a Universal Gamut Mapping Algorithm*, Ph.D. Thesis, University of Derby, 1998.

7. K.E. Spaulding, R.N. Ellson, and J.R. Sullivan, UltraColor: A New Gamut Mapping Strategy, *SPIE Proceedings*, **2414**: 61–68 (1995).

8. H. Motomura, Categorical Color Mapping for Gamut Mapping II – Using Block Average Image, *IS&T/SPIE Electronic Imaging '99, Color Imaging: Device Independent Color, Color Hardcopy, and Graphic Arts IV*, San Jose: 108-119 (1999).

9. L.W. MacDonald, Gamut Mapping in Perceptual Colour Space, *Proceedings of 1st IS&T/SID Color Imaging Conference*, Scottsdale:193–196 (1993).

10. CIE, The CIE 1997 Interim Colour Appearance Model (Simple Version), CIECAM97s, CIE Pub. 131 (1998).

11. M.C. Stone and W.E. Wallace, Gamut Mapping Computer Generated Imagery, *Graphics Interface '91*, pp. 32-39 (1991).

12. G.J. Braun and M.D. Fairchild, Gamut Mapping for Pictorial Images, *TAGA Proceedings*: 645-660 (1999).

13. G.J. Braun, F. Ebner, and M.D. Fairchild, Color Gamut Mapping in a Hue-Linearized CIELAB Color Space, *Proceedings of IS&T/SID 6th Color Imaging Conference*, Scottsdale: 163-168 (1998).

14. P. Hung and R.S. Berns, Determination of Constant Hue Loci for a CRT Gamut and Their Predictions Using Color Appearance Spaces, *Color Res. and Appl.*, **20**: 285-295 (1995).

15. F. Ebner and M.D. Fairchild, Finding Constant Hue Surfaces in Color Space, *Proceedings of SPIE, Color Imaging: Device-Independent Color, Color Hardcopy, and Graphic Arts III*, **3300-16**: 107-117 (1998).

16. G. Marcu, Gamut Mapping in Munsell Constant Hue Sections, *Proc. of IS&T/SID 6th Color Imaging Conference*, Scottsdale: 159-162 (1998).

17. J.J. McCann, Color Gamut Measurements and Mappings: The Role of Color Spaces, *IS&T/SPIE Electronic Imaging '99, Color Imaging: Device Independent Color, Color Hardcopy, and Graphic Arts IV,* San Jose: 68-82 (1999).

18. F. Ebner and M.D. Fairchild, "Development and Testing of a Color Space (IPT) with Improved Hue Uniformity", *Proceedings of the 6th IS&T/SID Color Imaging Conference*, Scottsdale: 8-13 (1998).

19. J. Holm, "Photographic Tone and Colour Reproduction Goals", *CIE Expert Symposium '96 on Colour Standards for Imaging Technology*: 51-56 (1996).

20. J. Holm, "A strategy for Pictorial Digital Image Processing (PDIP)", *Proceedings of the 4th IS&T/SID Color Imaging Conference*, Scottsdale: 194-201 (1996).

21. W.S. Torgerson, Chapter 9: The Law of Comparative Judgment, *Theory and Methods of Scaling*, Wiley, New York, 1967.

22. C.J. Bartleson and F. Grum, Optical Radiation Measurements, Vol. 5: Visual Measurements, Academic Press, 1984.

Table 1. Description of the gamut-mapping algorithms used in this study.

Algorithm	Lightness Compression	Chroma Compression	Image- or Device-Dependent (Lightness /Chroma)
LIN_LIN	Linear	Linear	Device/Device
GCUSP	Gaussian-Weighted Linear	Linear	Device/Device
SIG_LIN	Sigmoidal	Linear	Image/Device
SIG_KNEE	Sigmoidal	Knee (90%)	Image/Device
SIG_CLP	Sigmoidal	Clipping	Image/Device
SIG_ ENHANCE	Sigmoidal	3-Piece Linear (sigmoid-like)	Image/Device
SIG_ IMGGAM	Sigmoidal	Knee (90%)	Image/Image
GENERIC	Sigmoidal	Knee (90%)	Device/Device

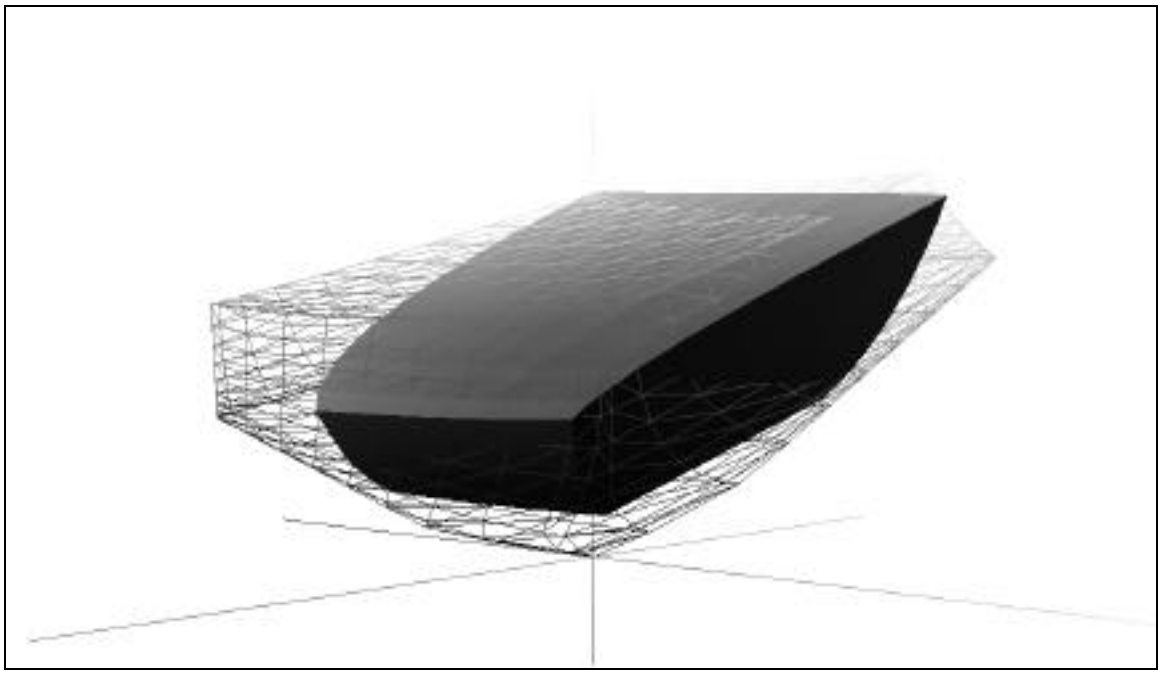

Figure 1. Illustration of the CIELAB gamut differences between imaging devices. The wireframe gamut is for a monitor and the solid gamut is for a thermal printer.

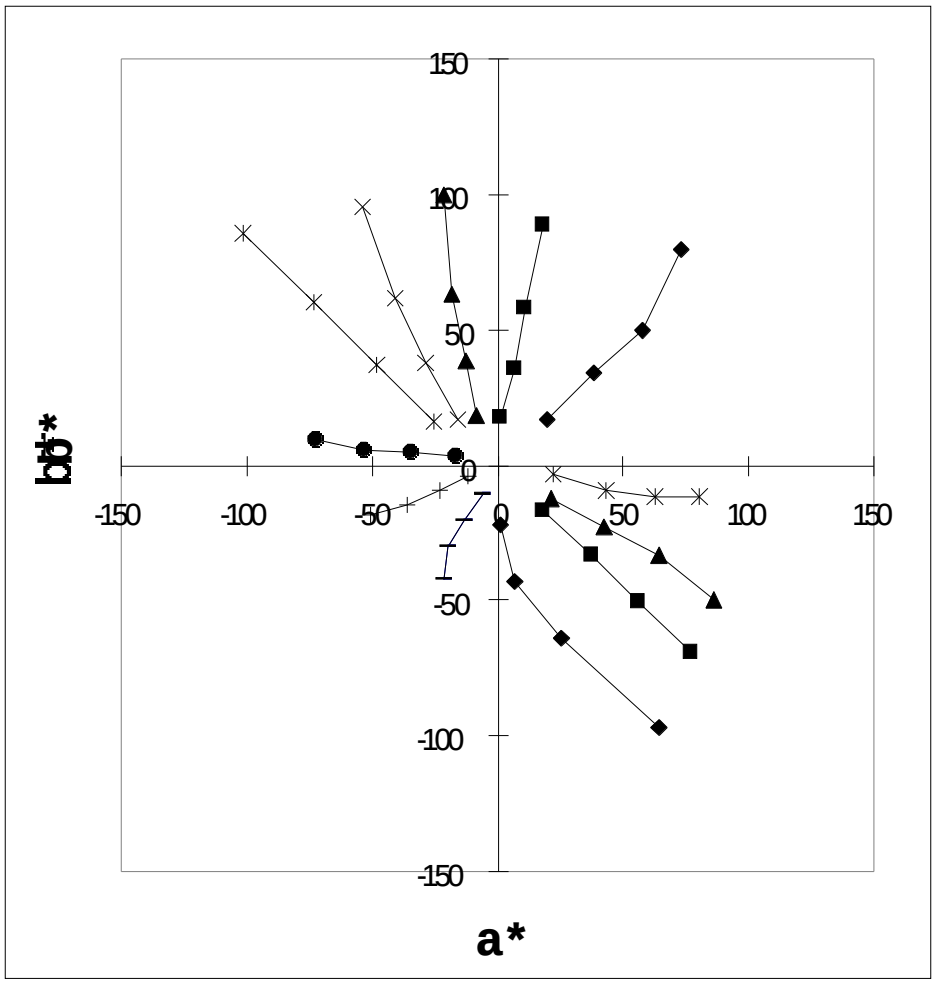

2a.

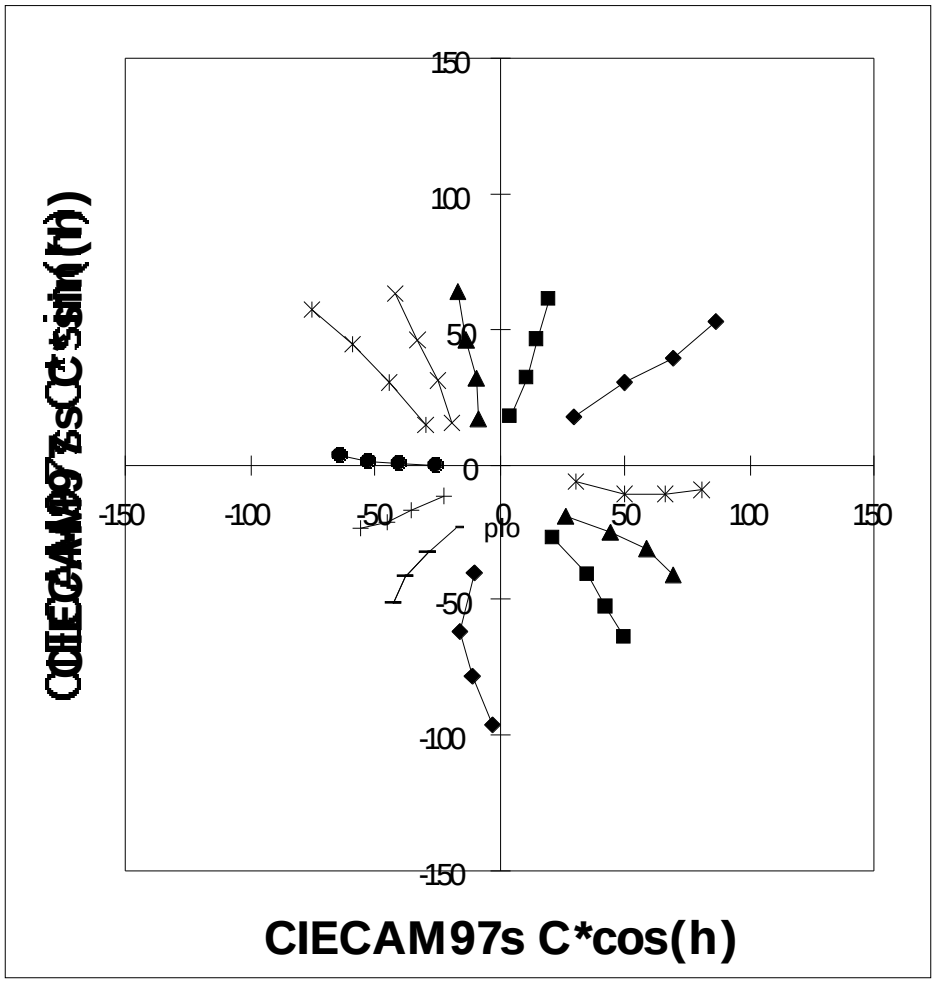

2b.

Figure 2a,b. Hung and Berns[12] lines of constant perceived hue plotted in (a) CIELAB and (b) CIECAM97s.

Figure 3. Illustration of four commonly used lightness rescaling functions. These functions map the high dynamic-range input lightness range into the reduced dynamic range of the output device.

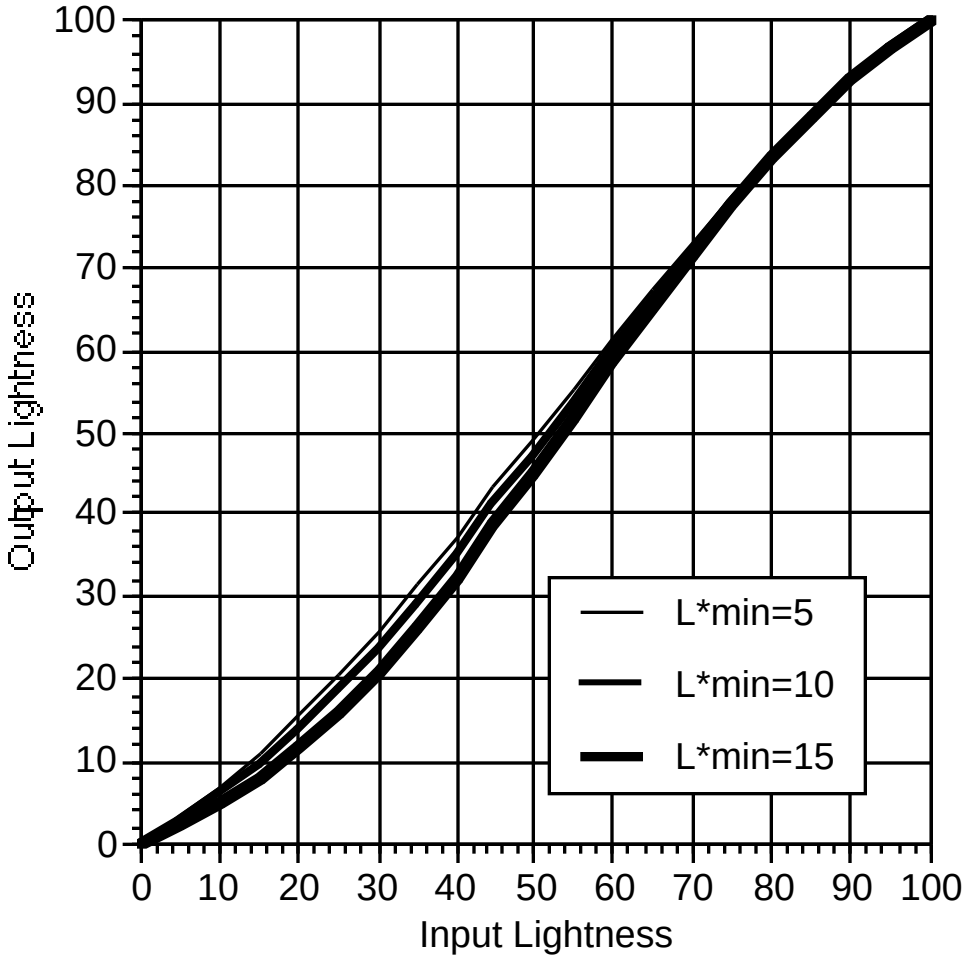
Output Lightness
Input Lightness
L*min=5
L*min=10
L*min=15
0
10
20
30
40
50
60
70
80
90
100

4a.

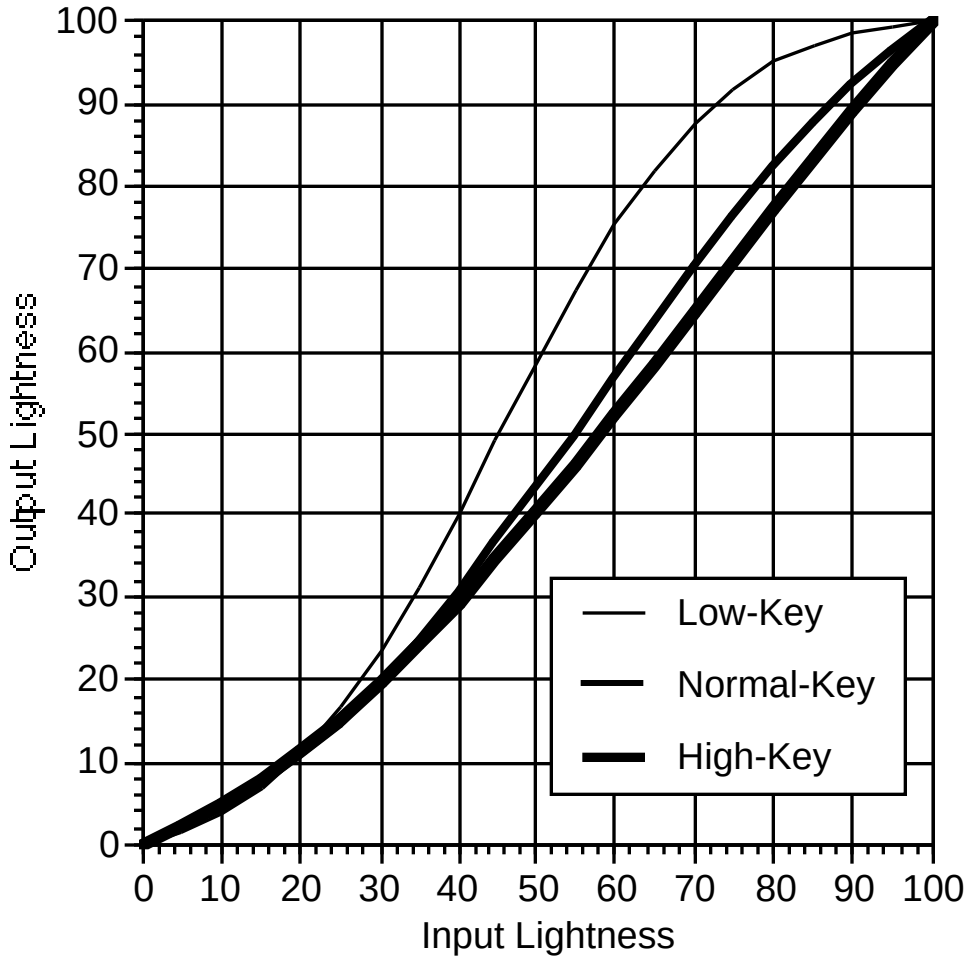

4b.

Figure 4a,b. Sigmoidal remappiung functions used to maintain perceived lightness contrast for (a) different output dynamic ranges and (b) different image content. (Note: The curves have been normalized to a range of {0-100} to illustrate the differences in contrast and curvature.)

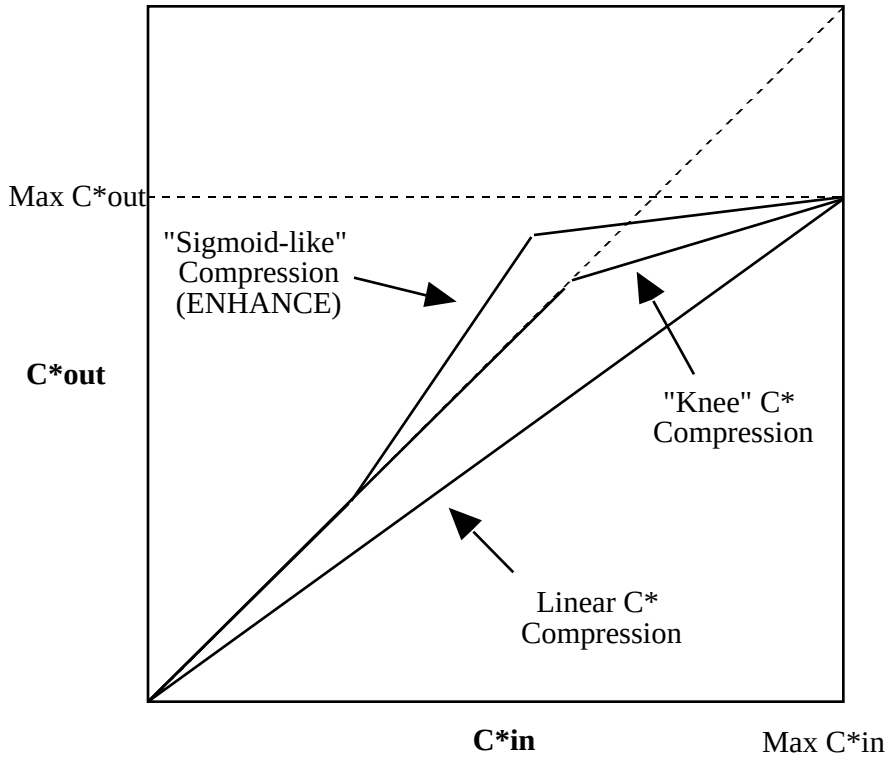

Figure 5. The chromatic compression functions used in these experiments.

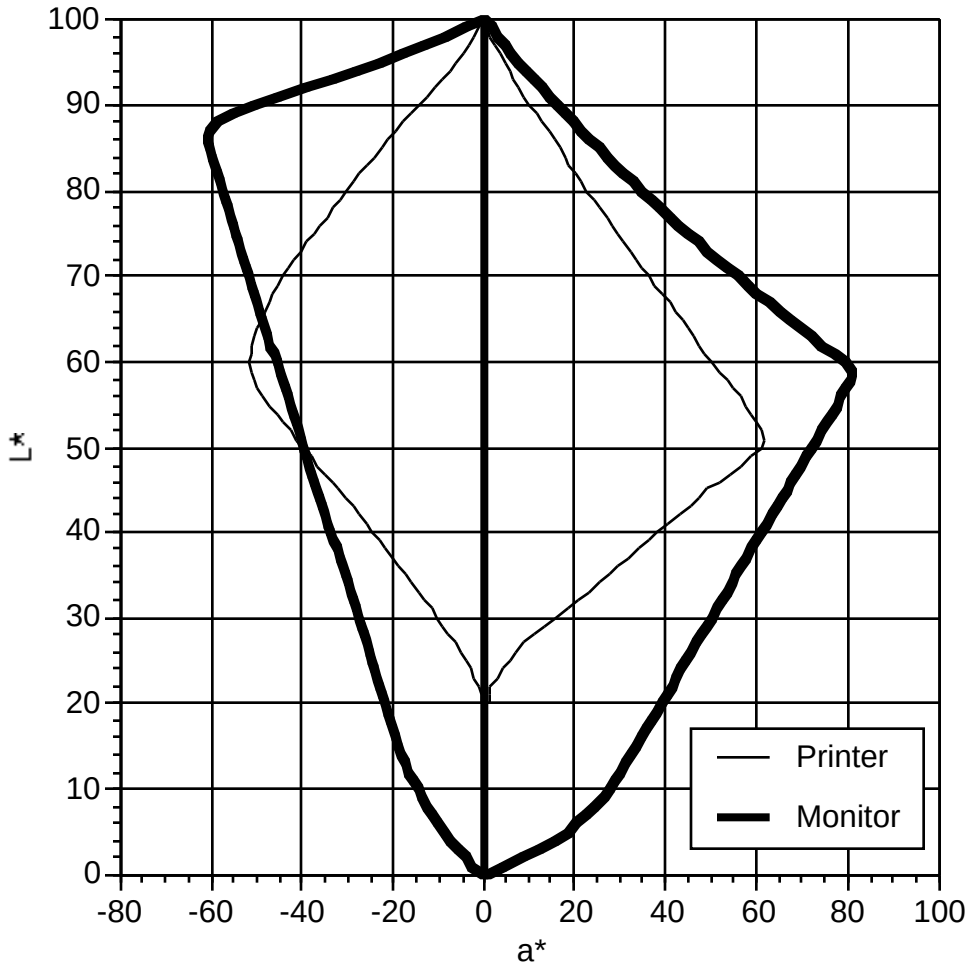
100
90
80
70
60
50
40
30
20
10
0
L*
-80
-60
-40
-20
0
20
40
60
80
100
a*
Printer
Monitor

6a.

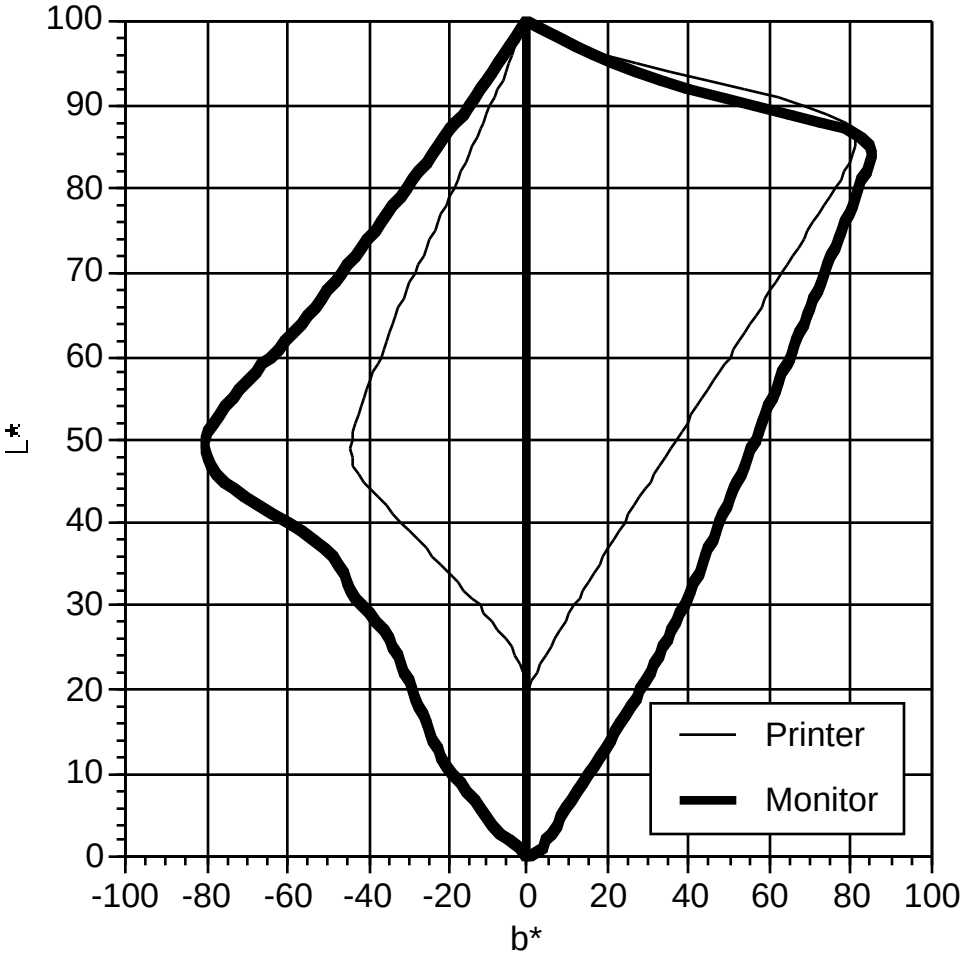

6b.

Figure 6a,b. Slices taken through the source (monitor) and destination (HP870Cxi inkjet printer) gamuts plotted on the Hung and Berns hue-linearized CIELAB a and b* axes.*

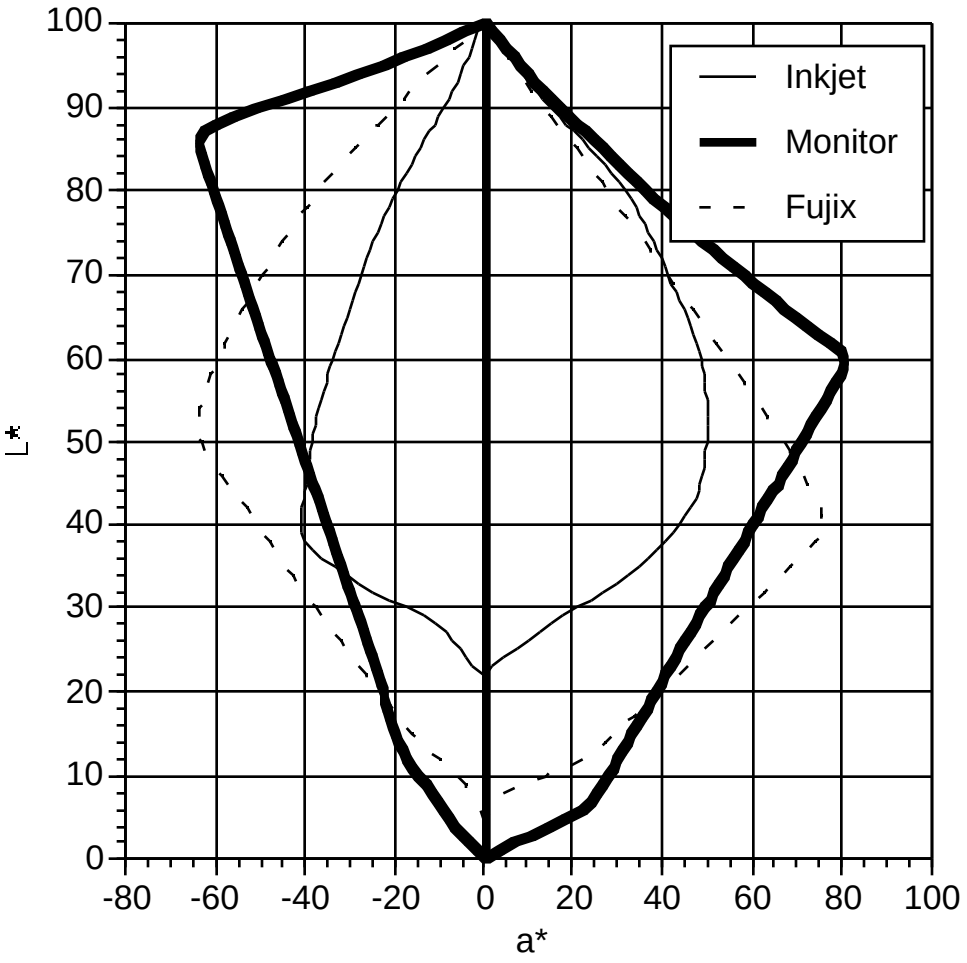
Inkjet
Monitor
Fujix
100
90
80
70
60
50
40
30
20
10
0
-80
-60
-40
-20
0
20
40
60
80
100
a*

7a.

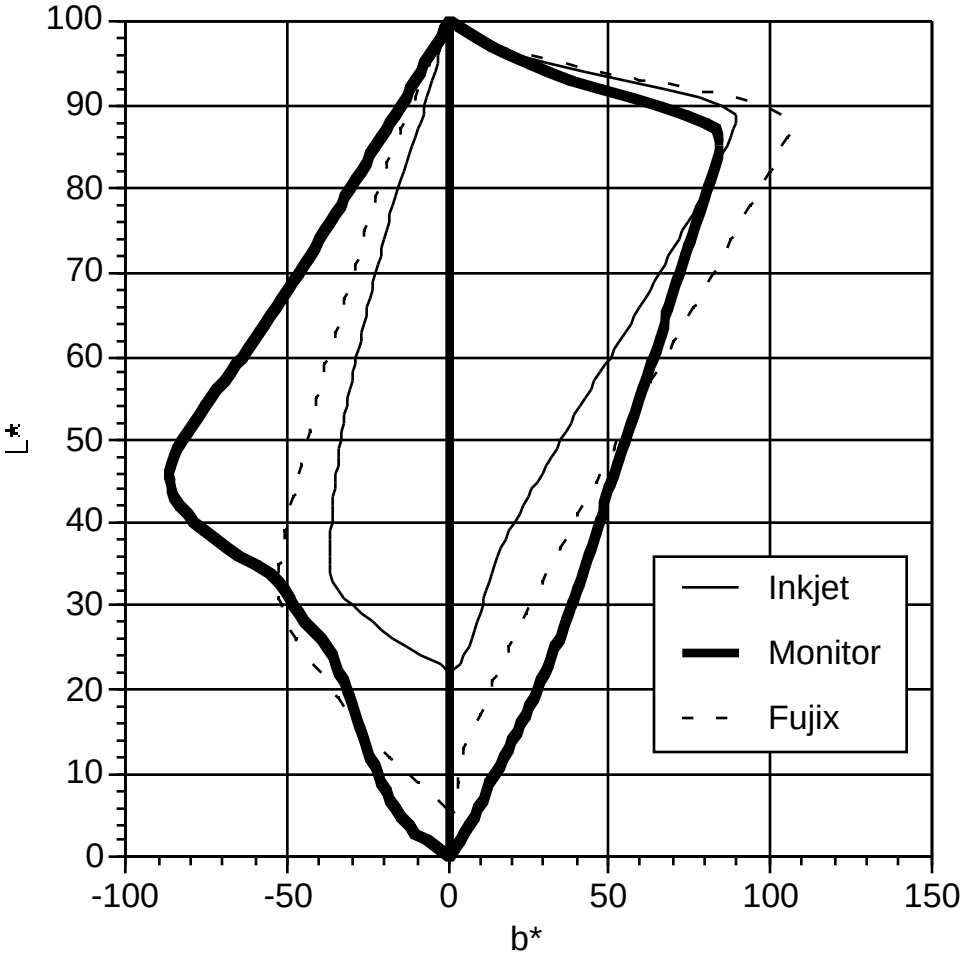

7b.

Figure 7a,b. Slices taken through the monitor and printer gamuts along the Hung and Berns hue-linearized CIELAB a and b* axes*

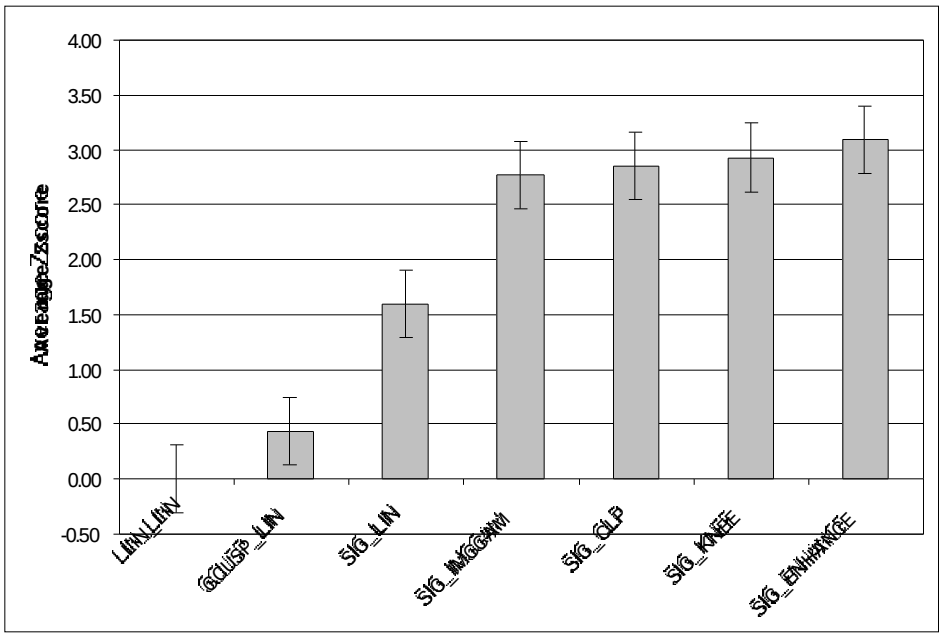

Figure 8. Interval scale results from the monitor-to-printer experiment, averaged across the seven images. Higher Z-score equals better performance.

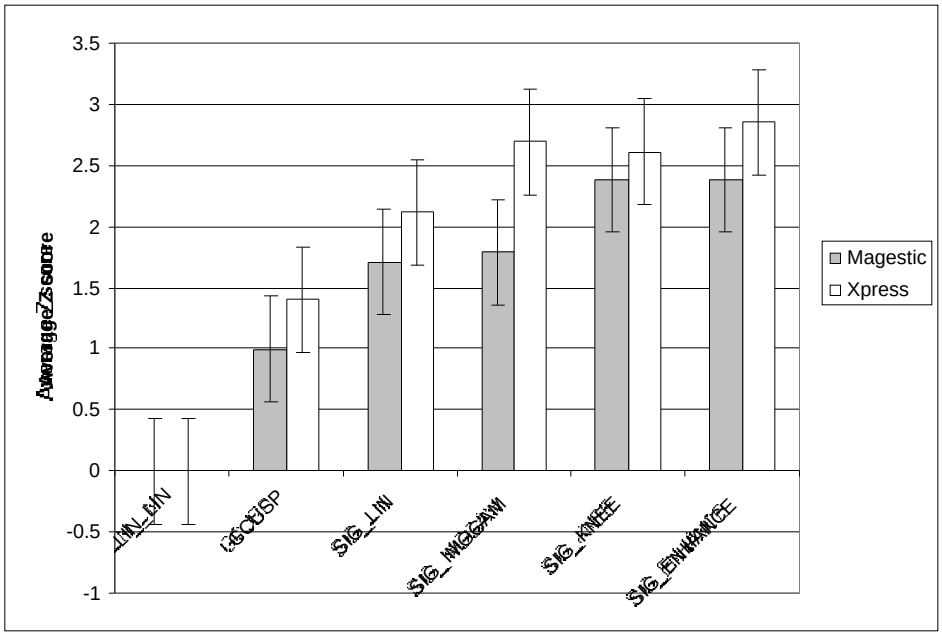

Figure 9. Interval scale results from the printer-to-printer experiment for the two destination printers, averaged across the four images.

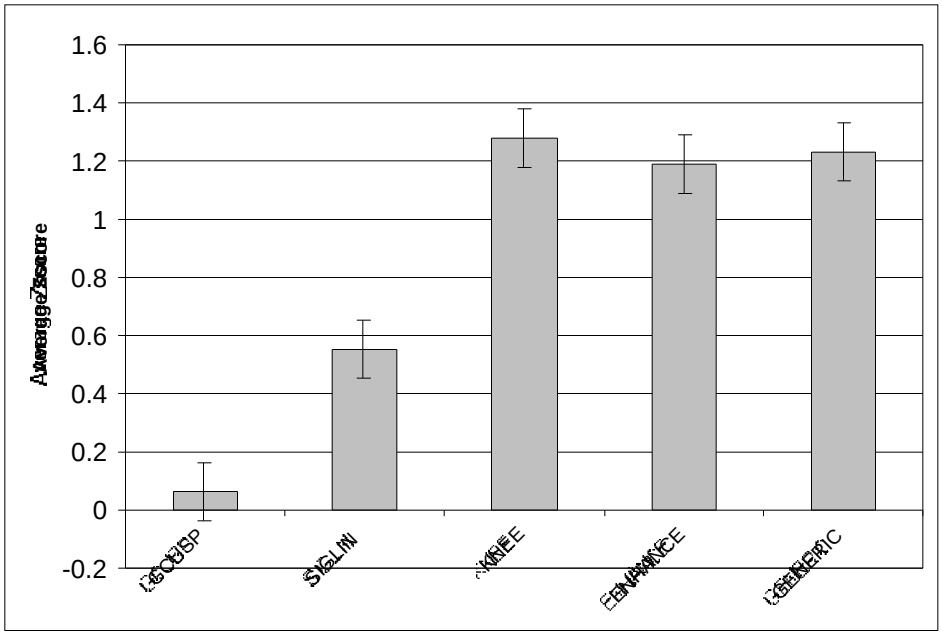

Figure 10. Interval scale results from the printer-to-printer softproof experiment, averaged across the eight images.